

PERIODIC PROGRESS REPORT NO. 1

for

SOLAR-CELL INTEGRAL COVER-GLASS DEVELOPMENT

for the period

February 10, 1967 to May 31, 1967

Contract No. NAS5-10319

Prepared by

TEXAS INSTRUMENTS INCORPORATED  
SEMICONDUCTOR-COMPONENTS DIVISION

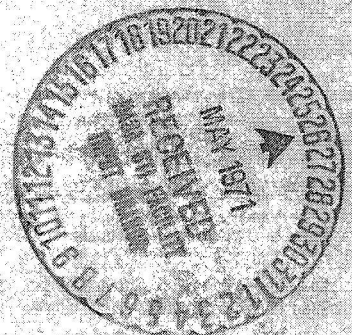
P. O. Box 5012  
Dallas, Texas 75222

FACILITY FORM 602

N71-73370	(THRU)
(ACCESSION NUMBER)	29
CR-178412	(CODE)
(PAGES)	
(NASA CR OR TMX OR AD NUMBER)	(CATEGORY)

for

NASA-GODDARD SPACE FLIGHT CENTER  
Glenn Dale Road  
Greenbelt, Maryland



PERIODIC PROGRESS REPORT NO. 1

for

## SOLAR-CELL INTEGRAL COVER-GLASS DEVELOPMENT

for the period

February 10, 1967 to May 31, 1967

Contract No. NAS5-10319

Prepared by

TEXAS INSTRUMENTS INCORPORATED  
SEMICONDUCTOR-COMPONENTS DIVISION

P. O. Box 5012  
Dallas, Texas 75222

for

NASA-GODDARD SPACE FLIGHT CENTER

Glenn Dale Road  
Greenbelt, Maryland

## SUMMARY

The object of this report is to present first-quarter progress on a 12-month research and development program for applying integral cover-glass coatings to silicon solar cells by radio-frequency sputtering. Integral quartz coatings up to 3.5 mils thickness have been deposited on standard solar cells at a rate of approximately 1200 Å/min by RF sputtering. The process variables that affect deposition rate have been investigated, with 2100 Å/min of quartz the highest rate obtained.

One-mil-thick integral coatings have been subjected to thermal shock from  $-196^{\circ}\text{C}$  to  $+100^{\circ}\text{C}$  with no apparent degradation or delamination from the solar cell. The stress of RF-deposited quartz films on silicon has been measured versus film thickness. The results show that maximum stresses involved ( $\cong 10^4$  psi) are much less than the compressive strength of  $\text{SiO}_2$  ( $> 1.6 \times 10^5$  psi); therefore the mechanical integrity of the films should be excellent.

Initial quartz depositions on standard solar cells yielded approximately 10 percent decrease in short-circuit current of the cell under  $100 \text{ mW/cm}^2$  tungsten light. This loss was expected, since the anti-reflective coating on the cells was silicon monoxide, which does not have the proper index of refraction to yield minimum reflection loss between Si and  $\text{SiO}_2$ . Also, the quartz films had no additional anti-reflective coatings on the top surface to minimize the reflection losses at this interface.

The anti-reflective coatings on either side of the quartz coating will be investigated during the course of the contract to minimize these reflection losses.

Radio-frequency sputtering has proven an excellent technique for depositing integral covers on silicon solar cells. This technique has the advantage of high deposition rate on low-stress, high-optical-quality quartz films. The substrate temperature can easily be maintained at less than  $200^{\circ}\text{C}$  throughout the deposition, which prevents damage to the solar-cell coating, contacts, and junction.

## TABLE OF CONTENTS

SECTION	TITLE	PAGE
I.	INTRODUCTION . . . . .	1
A.	Objective . . . . .	1
B.	Scope of Work . . . . .	1
II.	TECHNICAL DISCUSSION . . . . .	2
A.	Background . . . . .	2
1.	Fused Glass . . . . .	2
2.	Spray Coatings . . . . .	2
3.	Thermal Decomposition . . . . .	2
4.	Reactive Sputtering . . . . .	3
5.	Electron-Beam Deposition . . . . .	3
6.	High-Vacuum Sputtering . . . . .	3
7.	RF Sputtering . . . . .	3
B.	Radio-Frequency Sputtering . . . . .	4
1.	Theory . . . . .	4
2.	Apparatus . . . . .	7
3.	Process Variables . . . . .	7
4.	Experimental Results . . . . .	12
C.	Anti-Reflective Coatings . . . . .	18
D.	Environmental Testing . . . . .	19
E.	Sample Fabrication . . . . .	21
III.	PROGRAM FOR NEXT THREE MONTHS . . . . .	23
IV.	CONCLUSIONS . . . . .	24
V.	REFERENCES . . . . .	25

## LIST OF ILLUSTRATIONS

FIGURE	TITLE	PAGE
1.	RF Sputtering Process . . . . .	5
2.	RF Sputtering System . . . . .	8
3.	Electrode Assembly for RF Sputtering System . . . . .	8
4.	Deposition Rate at Two RF Input Power Levels as a Function of Magnetic Field Intensity . . . . .	9
5.	Variation of Deposition Rate Across Substrate Holder (Film Thickness Distribution) . . . . .	10
6.	Solar Cell I-V Characteristic Before and After Integral Quartz Coating . . . . .	13
7.	Solar Cell I-V Characteristic Before and After Integral Quartz Coating . . . . .	14
8.	Solar Cell I-V Characteristic Before and After Integral Quartz Coating . . . . .	15
9.	Stress versus Quartz-Film Thickness . . . . .	17
10.	I-V Curve Before and After Quartz Coating and After Thermal Shock . . . . .	20
11.	Solar Cell I-E Characteristic After Integral Quartz Coating . . . . .	22

## SECTION I

### INTRODUCTION

#### A. OBJECTIVE

The objective of this contract is to conduct a year's research and development program for applying integral cover-glass coatings to silicon solar cells by radio-frequency sputtering. The primary objectives for applying integral coatings to solar cells are: (1) to eliminate adhesive between cell and cover glass which (2) removes the requirement for ultraviolet rejection filters on under side of cover glass; (3) to increase power-to-weight ratio of cell/cover-glass assembly on missions which require less than 6-mil filters; (4) to reduce cost of present solar-cell-cover-glass combination. It is advantageous to eliminate the adhesive, since most adhesives darken under ultraviolet (u-v) radiation and are limited to a maximum temperature range of approximately 200°C. It has been demonstrated that radiation damage in silicon solar cells can be annealed out by subjecting the cell to approximately 400°C for brief periods.<sup>1/</sup>

#### B. SCOPE OF WORK

This development program involves deposition of integral quartz coatings directly on silicon solar cells by radio-frequency sputtering. Coatings, to be applied directly to the cell without subjecting it to temperatures in excess of 500°C, are to be in the thickness range of < 1 to 20 mils. Integral coated cells will be tested both optically and environmentally with conventional 6-mil 7940 quartz cover-slide cells as a control group. The program should yield an integral cover-glassed solar cell which pricewise is competitive under present-day production methods. Integrally cover-glassed sample cells will be supplied to NASA on scheduled dates during the contract.

## SECTION II

### TECHNICAL DISCUSSION

#### A. BACKGROUND

Protective covers are required for silicon solar cells on space-flight missions to assure protection against radiation damage and provide thermal control of the spacecraft. Various techniques have been used to apply the covers to the cells. Protective covers for Telstar satellite cells were mechanically attached to the cells.<sup>2/</sup> Nearly all the later satellites used cells whose protective covers were attached with an adhesive. Various protective covers and adhesives have been used, depending on each flight's radiation environment and temperature extremes.

In recent years work has been directed at applying the cover glass directly to the solar cell without employing adhesives. A brief discussion of techniques utilized in applying insulator films directly to silicon is presented below for review.

##### 1. Fused Glass

NASA Contract NAS 5-3857 (4 May 1964 to 4 November 1964) was a program to develop and produce integral glass coatings for solar cells. A limited amount of success was achieved with the coatings, which were applied in glass-slurry form and fused to the cell at a temperature between 850°C and 950°C. Major disadvantage of the procedure was that the solar-cell diffusion and contact procedures had to be modified to prevent this high-temperature fusing cycle from drastically degrading the cells.

##### 2. Spray Coatings

Spray coatings have been announced by Lockheed,<sup>3/</sup> but the advantages or exact properties of this coating are not explicitly known throughout the industry.

##### 3. Thermal Decomposition

The thermal-decomposition process involves passing an inert gas, as a carrying vapor, from the deposition agent over a heated substrate. The decomposing vapor deposits a film on the substrate. A large number of silanes have been used at Texas Instruments with deposition temperatures in the range of 400°C to 900°C. Major disadvantage of this technique is the relatively high deposition temperature and the relatively poor film quality for thick ( $> 10,000 \text{ \AA}$ ) depositions.

#### 4. Reactive Sputtering

SiO<sub>2</sub> films in excess of 1.0 mil in thickness have been deposited on silicon by reactive sputtering. Silicon is used as the cathode in this process, and the sputtering operation in an oxygen-rich atmosphere deposits SiO<sub>2</sub> on the substrate.

Reactively sputtered SiO<sub>2</sub> can produce a thick film which is exceptionally smooth; however, sputtering rate must be kept below 200 Å/min, and substrate temperature must be kept above 500°C. Consequently, 21 hours of continuous deposition would be required for producing a good film 1 mil in thickness. At higher deposition rates and lower substrate temperatures this process produces incompletely oxidized films of low density, thereby limiting reactive sputtering, for most practical applications, to deposition of relatively thin films at high temperatures.

#### 5. Electron-Beam Deposition

SiO<sub>2</sub> films in excess of 5.0 mils have been deposited by focused-electron-beam techniques, using quartz as the source material. A major advantage of this technique is the substrate's relatively low temperature during deposition. Normally the substrate temperature may be below 50°C during the deposition to minimize thermal-stress problems. A disadvantage of this technique is the degree of control required to maintain a low evaporation rate in order to keep large particles of quartz from being evaporated. Highly strained films, which readily strip from silicon substrate, are commonly deposited with this technique unless a very low deposition rate (normally < 300 Å/min) is utilized.

#### 6. High-Vacuum Sputtering

NASA Contract NAS 5-10236 (starting date, June, 1966) was initiated to investigate integral cover-glass techniques for silicon solar cells. Several deposition techniques have been investigated during this contract, but the best reported results were obtained by high-vacuum sputtering. This technique has reportedly yielded films with excellent optical and mechanical characteristics; however, the rate at which the films are deposited is very low (average SiO<sub>2</sub> deposition rate is 100 Å/min).<sup>4/</sup>

#### 7. RF Sputtering

The subject contract is to investigate radio-frequency sputtering specifically for integral cover-slide application. Although virtually any insulator can be deposited by this technique, only Corning 7940 fused silica will be used for integral cover-glass material. RF sputtering will also be utilized to investigate silicon nitride for anti-reflective coatings between the silicon solar cell and the integral SiO<sub>2</sub> coating.



It has been demonstrated at Texas Instruments that complex thin films, such as pyrex, deposited by RF sputtering have physical and chemical properties basically identical with the parent bulk material. RF sputtering has the advantage of high deposition rates ( $> 1000 \text{ \AA}/\text{min}$  for  $\text{SiO}_2$ ) and low substrate temperatures ( $< 200^\circ\text{C}$ ). RF-deposited integral quartz films of 1 to 2 mils thickness have successfully passed five thermal shock cycles from  $-196^\circ\text{C}$  to  $+100^\circ\text{C}$  with no mechanical or physical deterioration or delamination from the solar cell.

## B. RADIO-FREQUENCY SPUTTERING

### 1. Theory

The term "sputtering" refers to the ejection of atoms from a material through the impact of ions with the atoms on the material's surface. The most common technique is to make the material to be sputtered a cathode in a low-pressure, dc glow discharge, utilizing an inert gas such as argon to form the plasma. Since almost the entire applied voltage is dropped across the ion sheath that surrounds the cathode (Crookes dark space), the cathode will be under bombardment by high-energy ions, a condition that results in sputtering of the cathode source. If a substrate is placed near the cathode, it can collect the sputtered atoms to form a film. Obviously the dc sputtering is applicable to the sputtering of conductors only. If an insulator is used for the cathode instead of a conductor, the positive charge which accumulates on the surface during ion bombardment cannot be neutralized, and sputtering ceases. Therefore an insulator cannot be applied directly by dc sputtering.

Since RF fields can penetrate insulators, the problem can be overcome by applying a high-frequency potential to the metal electrode behind the insulator.<sup>5/</sup> A simplified electrode system, patterned after Butler and Kino,<sup>6/</sup> and serving to illustrate the sputtering mechanism, is seen in Figure 1. This idealized electrode system consists of two parallel plates similar to the electrodes of a parallel-plate capacitor. A radio-frequency potential is applied to the capacitor by grounding one electrode and impressing the voltage on the other. An insulating sheet is placed between the plates near the ungrounded electrode, so that the electric field between the electrodes penetrates the insulator.

As the potential of the ungrounded electrode swings positive and negative, induced charges appear on the inside surface of the insulator. Positive and negative particles in the ionized argon plasma are attracted to and repelled from the insulator surface by the induced surface charge. During the positive half-cycle, electrons are collected on the surface of the insulator; during the negative half-cycle, positively charged argon ions are collected on the surface. Since the mobility of the electrons in the plasma is much greater than that of the argon ions, more electrons than positive argon ions are collected on the insulator surface during initial RF cycles.

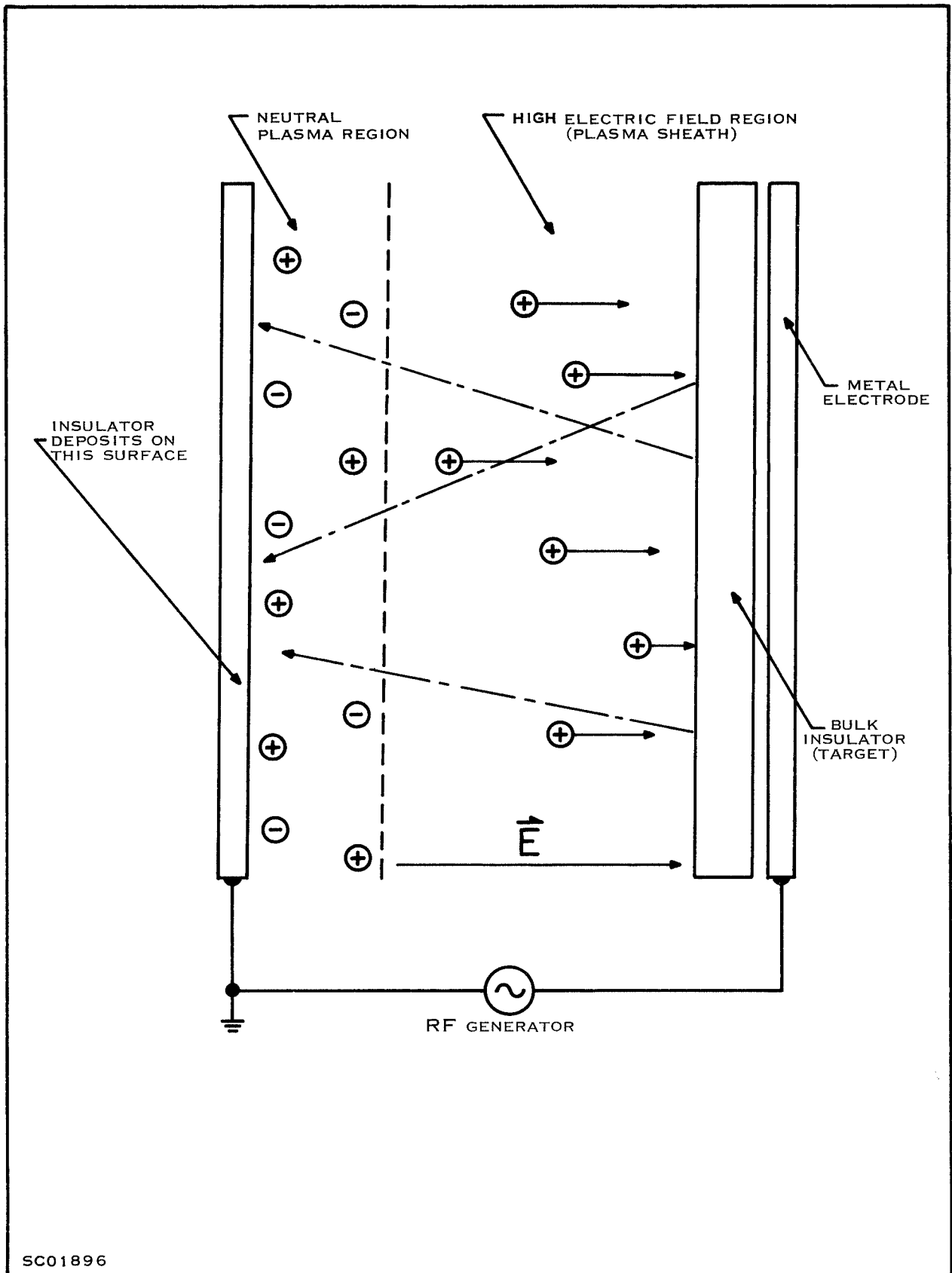


Figure 1. R-F Sputtering Process

The result is an accumulation of negative charge on the insulator surface which lowers the potential of the surface with respect to the plasma potential. This further increases the accelerating voltage of the argon ions which are swept out of the plasma region. Since the accelerating voltage is typically 3000 V peak-to-peak, the argon ions acquire considerable kinetic energy before reaching the insulator. When the massive argon ions strike the insulator surface the sputtering process occurs, resulting in deposition of the insulator on surfaces inside the vacuum system. In a well-designed electrode assembly most of the insulator material will be deposited on the electrode surface directly opposite the insulator surface. Therefore the substrates requiring the thin insulating film are mounted on the grounded electrode.

As this surface simply needs to supply a ground for the radio-frequency circuit, complex arrangements can be provided to control the substrate temperature and still maintain ground requirements for the radio-frequency circuit.

Applications of radio-frequency sputtering to insulators have produced excellent results unattainable by any other method.<sup>7/</sup> Deposition rates for silica ( $\text{SiO}_2$ ) of 2000 Å per minute have been achieved with excellent film properties. Table I<sup>8/</sup> shows some of the various types of glasses and other insulators which have been deposited by RF sputtering.

Table I. Relative RF Sputtering Rates for Various Materials at Several Thousand Volts Peak-to-Peak

Material	Composition	Relative Rates
Fused quartz	( $\text{SiO}_2$ )	1.0
GSC-1 glass	(5% $\text{Al}_2\text{O}_3$ , 10% $\text{B}_2\text{O}_3$ , 85% $\text{SiO}_2$ )	0.58
Pyrex 7740	(80.5% $\text{SiO}_2$ , 12.9% $\text{B}_2\text{O}_3$ , 3.8% $\text{Na}_2\text{O}$ , 2.2% $\text{Al}_2\text{O}_3$ , 0.4% $\text{K}_2\text{O}$ )	0.42
191 CP glass	(16% $\text{Al}_2\text{O}_3$ , 7% $\text{CaO}$ , 77% $\text{SiO}_2$ )	0.30
Alumina	( $\text{Al}_2\text{O}_3$ )	0.30
Mullite	( $\text{Al}_6\text{Si}_2\text{O}_{13}$ )	0.30
Boron nitride	(BN)	0.25

## 2. Apparatus

Several RF sputtering systems have been constructed during the past year at Texas Instruments. Figure 2 is a photograph of the apparatus presently in use on this contract. The vacuum system, associated pressure controllers, power supplies, and RF generator can be seen.

In Figure 3, a photograph of the electrode assembly, the circular quartz target can be seen approximately one inch below the substrate holder. Infrared heating lamps and cooling coils for the substrate can be seen. Cooling coils for the cathode-target assembly are also visible.

## 3. Process Variables

The deposition rate of an RF sputtering system is dependent on several variables, the most critical of which are listed in this section.

### a. Ionization Gas

The sputtering yield (number of sputtered atoms per incident ion) depends upon the mass of the ion. Argon is commonly used due to its relatively high mass (with respect to helium) and comparatively low cost. Deposition rates as high as 2200 Å/min of SiO<sub>2</sub> have been observed at Texas Instruments, with argon as the ionization gas. Substitution of krypton for argon on one run yielded an increase of 22 percent in deposition rate of SiO<sub>2</sub>. Neon,<sup>9</sup> helium, and xenon<sup>10</sup> ions have also been investigated by other scientists. Since the purity of the ionization gas is critical to the deposition rate, argon gas of 99.999 percent purity is currently being used for SiO<sub>2</sub> depositions on this contract.

### b. Superposed Magnetic Field

It was observed by Davidse and Maissel of IBM that a superposed magnetic field greatly increased the deposition rate. Figures 4 and 5<sup>8</sup> demonstrate, respectively, the effect of the superposed field on the deposition rate and the variation of deposition rate across the substrate holder. The electrons interact with the magnetic field, which causes the electrons to spiral around the lines of force, thereby increasing the ion density and deposition rate.

As can be seen in Figure 4, the higher power-input conditions require higher magnetic fields to obtain maximum deposition rate. The highest magnetic field used to date on depositions of quartz on solar cells has been 150 gauss. Additional electromagnets will be added to the system to increase the deposition rate as the input power is increased.

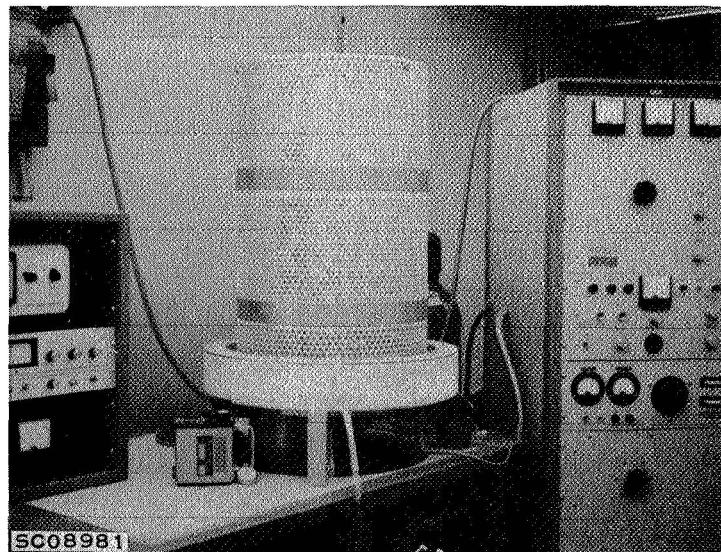


Figure 2. RF Sputtering System

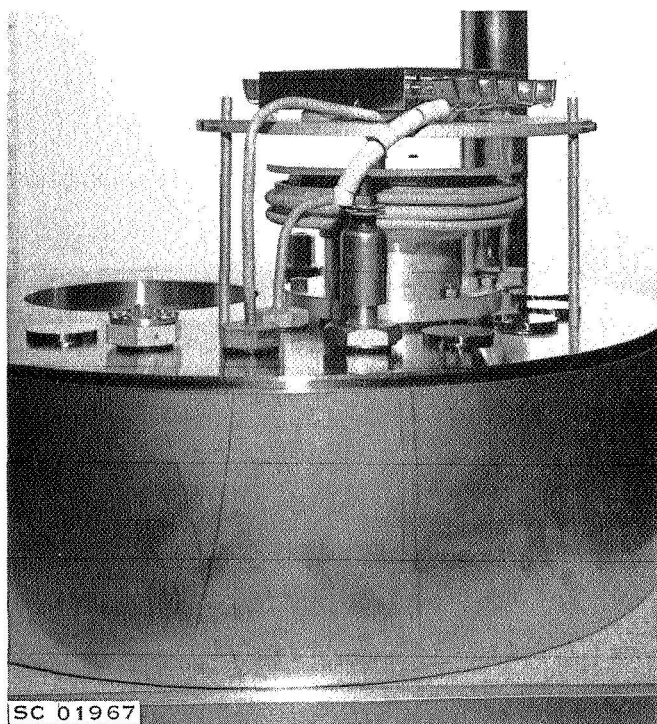


Figure 3. Electrode Assembly for RF Sputtering System

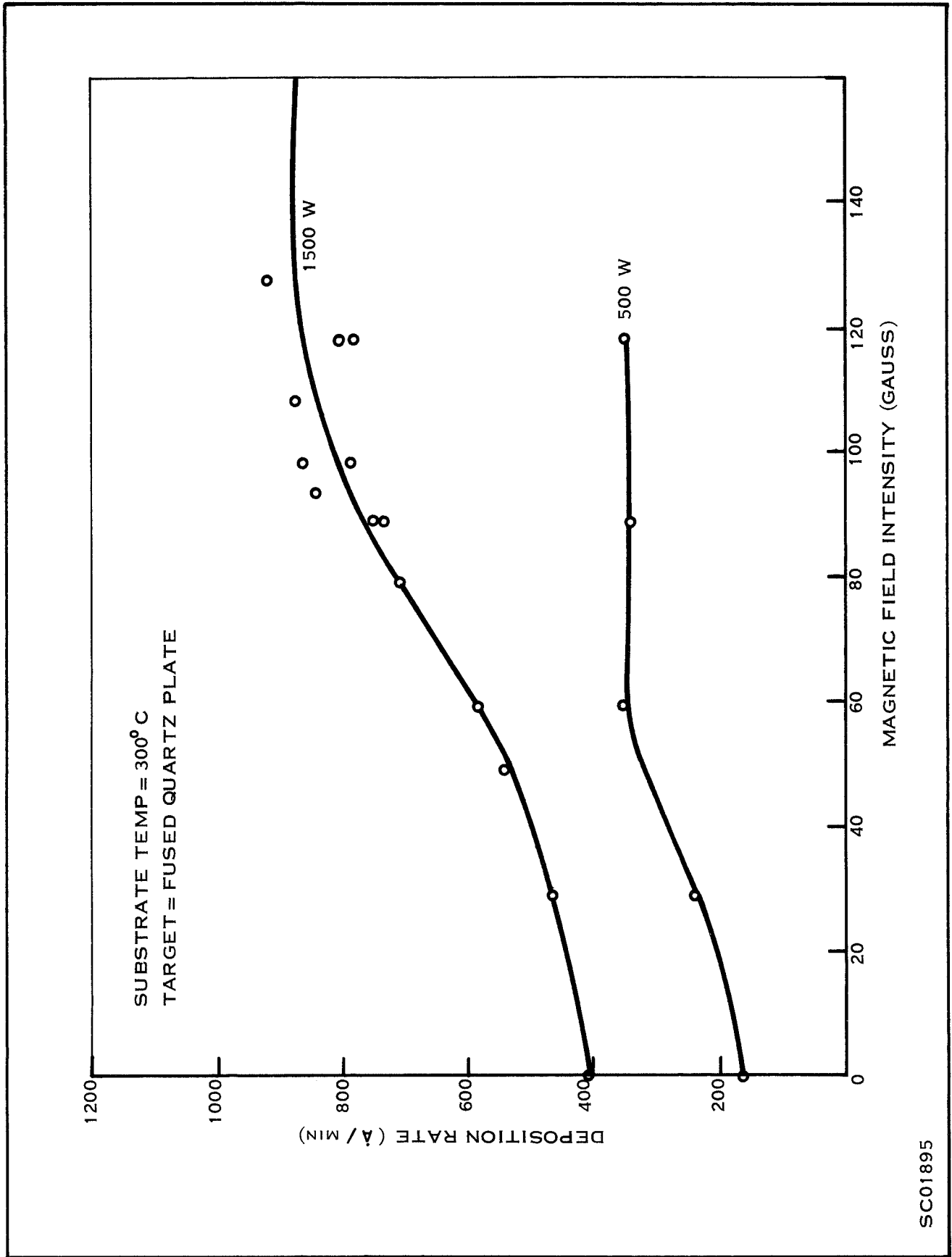


Figure 4. Deposition Rate at Two RF Input Power Levels as a Function of Magnetic-Field Intensity

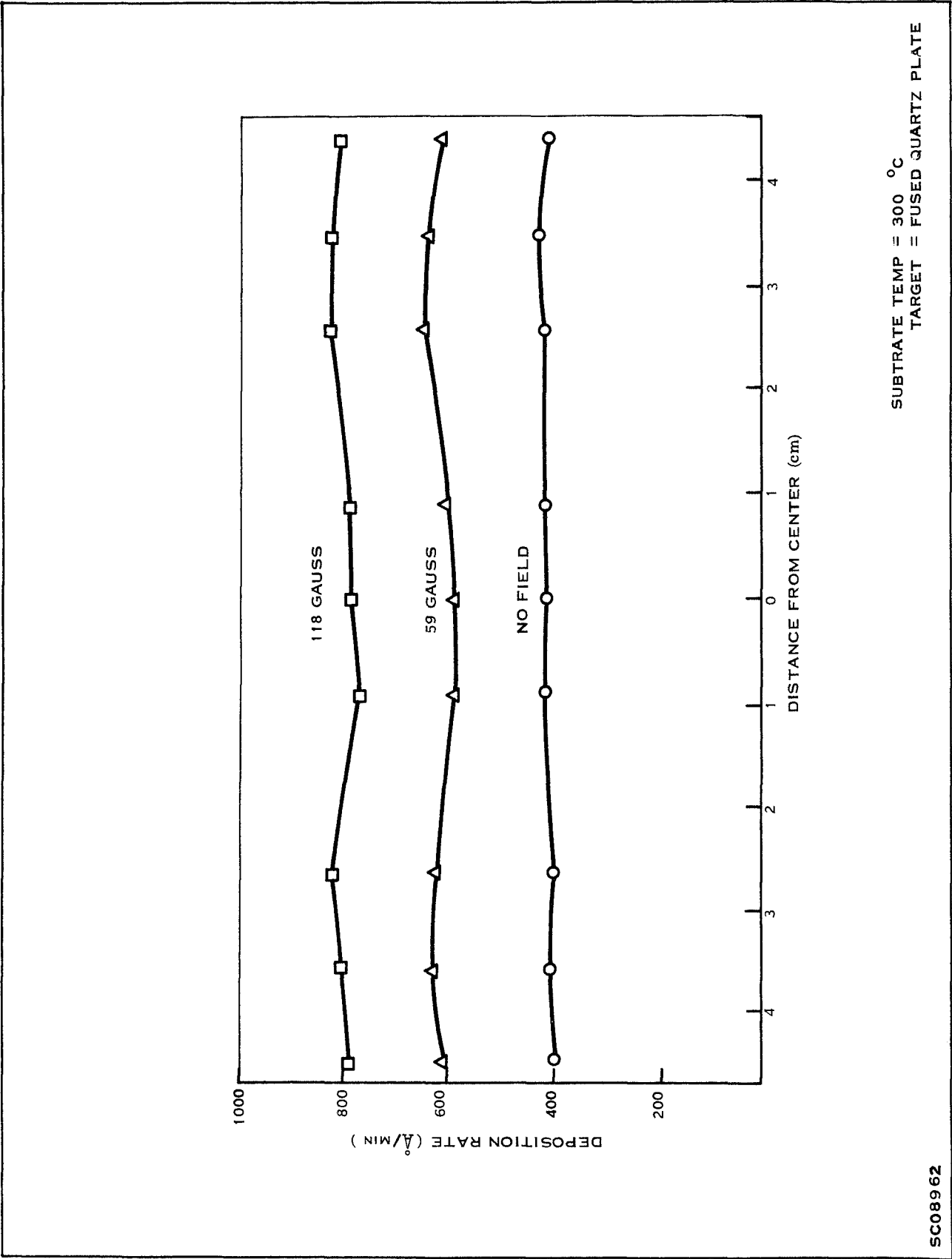


Figure 5. Variation of Deposition Rate Across the Substrate Holder (Film Thickness Distribution)

c. Substrate Temperature

Substrate temperature directly affects the deposition rate and film quality. Depositions have been made with substrate temperatures ranging from  $-196^{\circ}\text{C}$  to  $+300^{\circ}\text{C}$ . The low-temperature films, while deposited at a very high rate, were very porous, of low density, and generally poor optically.

Films deposited at  $30^{\circ}\text{C}$  appear identical physically with  $300^{\circ}\text{C}$  films; however, the deposition rate for the  $30^{\circ}\text{C}$  film is approximately 30 percent higher. Therefore depositions are normally made with approximately  $30^{\circ}\text{C}$  substrate temperature.

d. Power Input

Power input is one of the primary factors governing deposition rate. Actually the power input per unit cathode area specifically determines the deposition rate.

For a fixed cathode area the deposition rate will increase up to certain power level, at which point saturation occurs and additional power input does not yield increased deposition rate.

The present sputtering system utilizes 1000-watt input into a 6-inch-diameter cathode (28.2 watts per square inch). The system is easily capable of 3000-watt input. Additional power input will be used to determine the saturation point and maximum deposition rate when proper cooling is installed in the system to minimize heating problems at the higher power levels.

e. Geometry of System

The system geometry determines both the maximum number of cells that can be coated in a single run and the maximum power input to obtain a given deposition rate. The substrate-to-source distance has been optimized to yield the maximum deposition rate and uniformity for the present geometry.

The present 6-inch-diameter cathode is capable of depositing films on 70  $1 \times 2$ -cm, three-grid solar cells. By increasing the target diameter to 10 inches, approximately 210  $1 \times 2$ -cm cells can be deposited in a single sputtering cycle. However, the power input must be increased to 2780 watts to obtain the same deposition rate with the 10-inch-diameter cathode as is being achieved with the 6-inch-diameter cathode and 1000 watts of input.



#### 4. Experimental Results

##### a. Processing

Work during the first quarter of the contract was directed primarily at optimizing the deposition rate and thickness uniformity. Supersil II grade quartz from Engelhard Industries was used on all depositions up to April 4, at which time the Corning 7940 fused-silica targets were received and utilized. There is no observable difference in deposition rate between the Supersil II and the 7940 targets. The 7940 target is required for all depositions on the contract. The Supersil II target was used only to optimize the processing variables in the contract's initial stages.

Highest deposition rate obtained on the contract to date has been 2100 Å/min, with approximately 25 percent uniformity over the working area of the substrate holder. The majority of the runs to date has averaged between 1200 and 1600 Å/min.

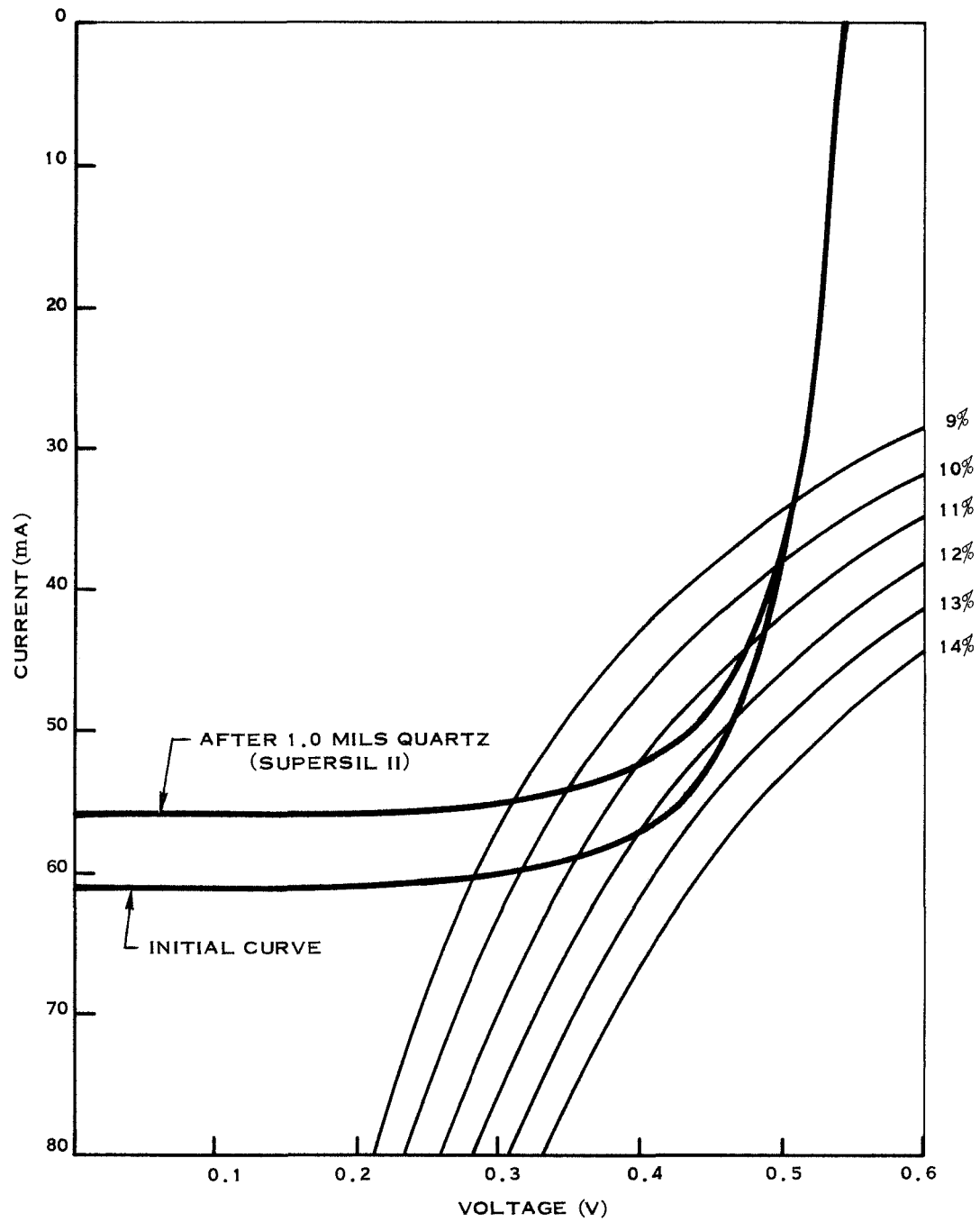
Initial runs were made to deposit films over 1.0 mil thick during this reporting period. The first eight-hour run yielded cells with 2.4 mils of quartz; a subsequent four-hour run on these cells produced total quartz thickness of 3.5 mils average. The 3.5-mil quartz coating had a pitted or "crazed" surface believed to have been caused by a small water leak in the substrate cooling system.

Figures 6, 7, and 8 show the I-V characteristics of typical cells under 100 mW/cm<sup>2</sup> tungsten before and after integral coatings of respectively 1.0, 2.4, and 3.5 mils thickness. Integral coatings were deposited on standard silicon monoxide coated cells with no additional anti-reflective coatings applied at the quartz-air interface. Since there is no appreciable change in spectral response of the cells after integral coating, the output curves are believed to be equivalent to 100 mW/cm<sup>2</sup> sunlight data. An attempt was made in May to obtain actual Table Mountain data on integral coated cells, but overcast conditions at the test site prevailed.

Approximately 700 solar cells have been fabricated specifically for this program. The I-E characteristic under 100 mW/cm<sup>2</sup> sunlight-equivalent tungsten light has been plotted for each cell.

##### b. Stress Analysis

To determine the stress of the integral films on the substrate, quartz coatings of from 0.6 to 1.8 mils thickness were deposited on 2 x 2-cm silicon solar cells of from 2.4 to 3.5 mils thickness. Coatings were deposited at a rate of from 1000 to 2000 Å/min. Subsequent to deposition of these thick films, considerable curvature of the cells was observed. Films were on the convex side of the substrates, indicating compressive stresses in the films. As the coefficient of thermal expansions for Si is several times greater than that for SiO<sub>2</sub>, and the actual deposition temperature at the



SC08493

Figure 6. Solar Cell I-V Characteristic Before and After Integral Quartz Coating

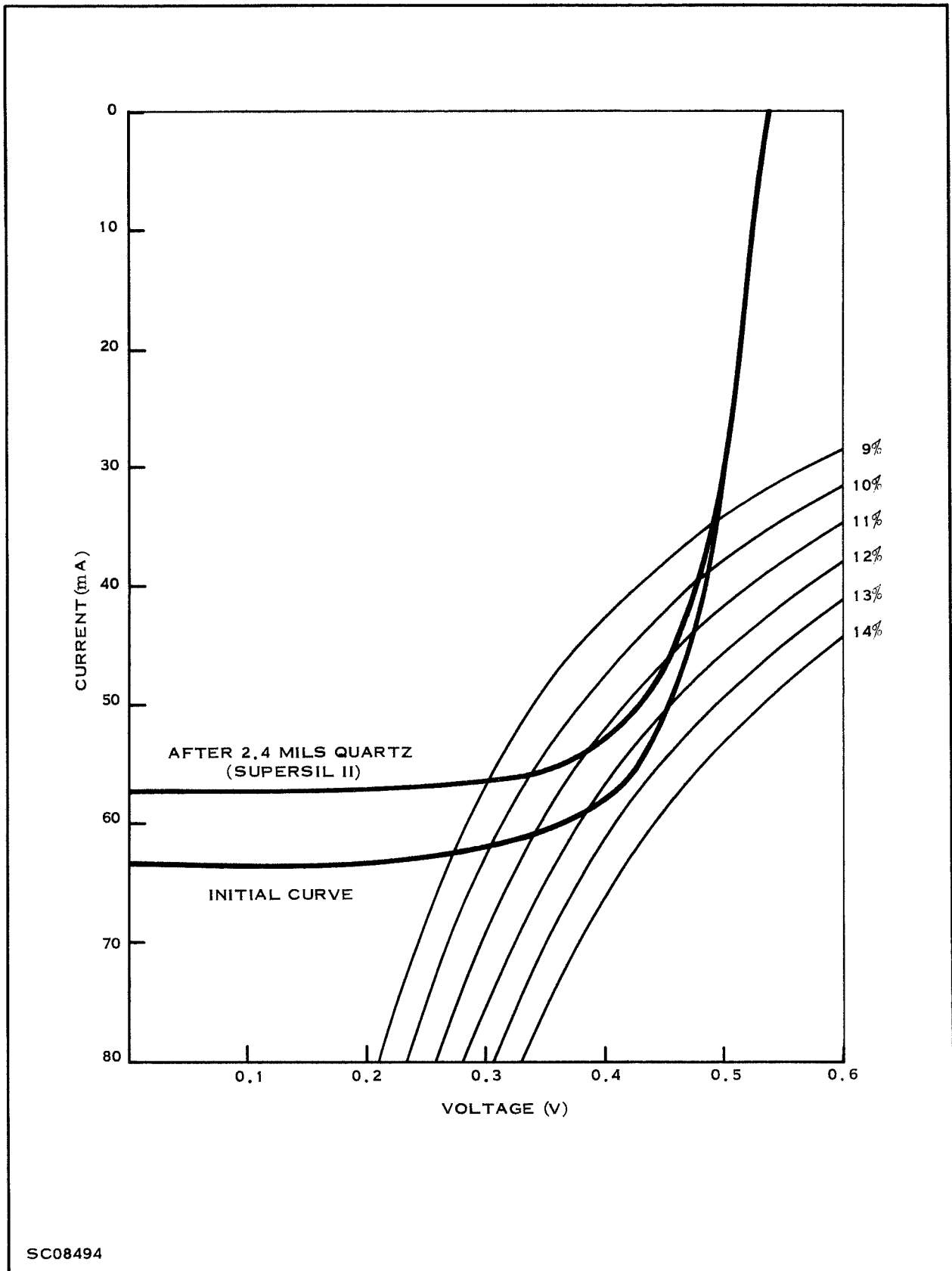
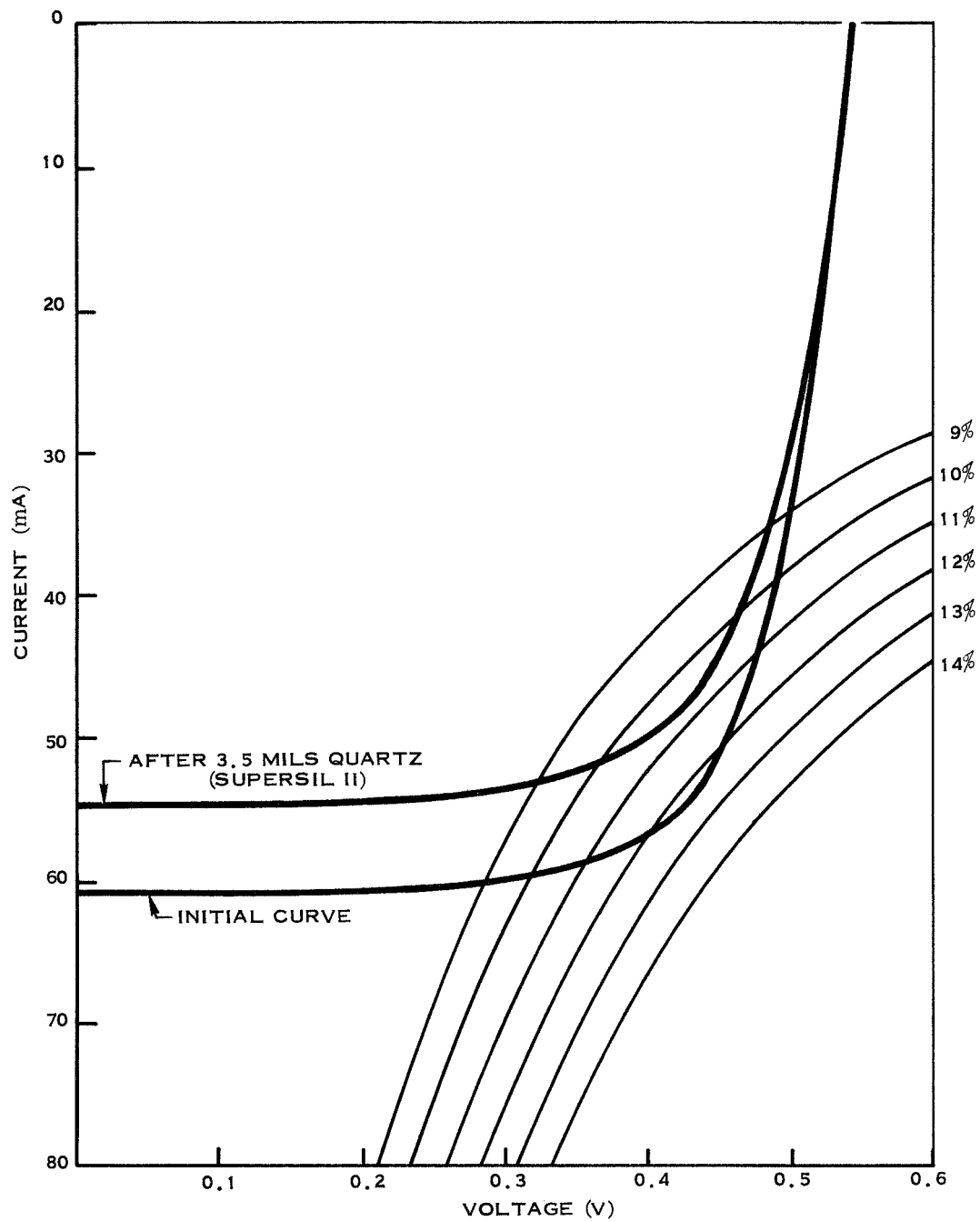


Figure 7. Solar Cell I-V Characteristic Before and After Integral Quartz Coating



SC08495

Figure 8. Solar Cell I-V Characteristic Before and After Integral Quartz Coating

growing surface is undoubtedly raised by the sputtering process, compressive stresses can be explained by thermal arguments. The magnitude of these stresses may be estimated from quantitative observations of the curvature.

Brenner and Senderoff<sup>11/</sup> have derived exact relationships between film stress  $S$ , substrate thickness  $t$ , film thickness  $d$ , and radius of curvature  $r$ , for various deposition configurations. Their equations differ substantially from those used by earlier workers<sup>12/</sup> in that they do not neglect the force required to bend the film, nor do they assume the elastic moduli of substrate and film to be equal. The exact equations are somewhat unwieldy, however, and for the configuration used here they suggest the two-term approximation

$$S = \frac{E_s t (t + Rd)}{6rd}$$

where  $E_s$  is the elastic modulus of the substrate and  $R$  is the ratio of the film modulus to that of the substrate,  $R = E_f/E_s$ . Brenner and Senderoff include an analysis of errors involved in this approximation which indicated deviations of less than 10 percent from the exact equations in the most extreme case encountered here.

Several cells were mapped for curvature by standing them on edge on an x-y micrometer stage and observing points along one edge with a microscope equipped with a cross-hair eyepiece. Precision of these measurements was  $\pm 0.01$  mil. Substrate and film thicknesses were observed at several points along each slice by the same optical technique. Results of these preliminary measurements are presented in Table II. It can be seen that the average film stresses are actually relatively low, all observed values being below  $10^4$  psi.

Table II. Preliminary Measurements

Slice	t (mil)	d (mil)	r (in)	S (psi)
11	2.88	0.64	10.6	6210
9	3.18	0.75	11.2	6130
5	3.45	0.95	13.3	4830
2	3.10	1.15	12.3	3600
3	2.42	1.86	10.4	1820

The other major feature of these results is that the stress systematically decreases with increasing film thickness. Figure 9 shows a semi-logarithmic plot of stress versus film thickness. The data are seen to be reasonably fitted by a straight line indicating an exponential decrease in stress with thickness. The fact that the stress decreases at a greater than linear rate shows that the total force involved

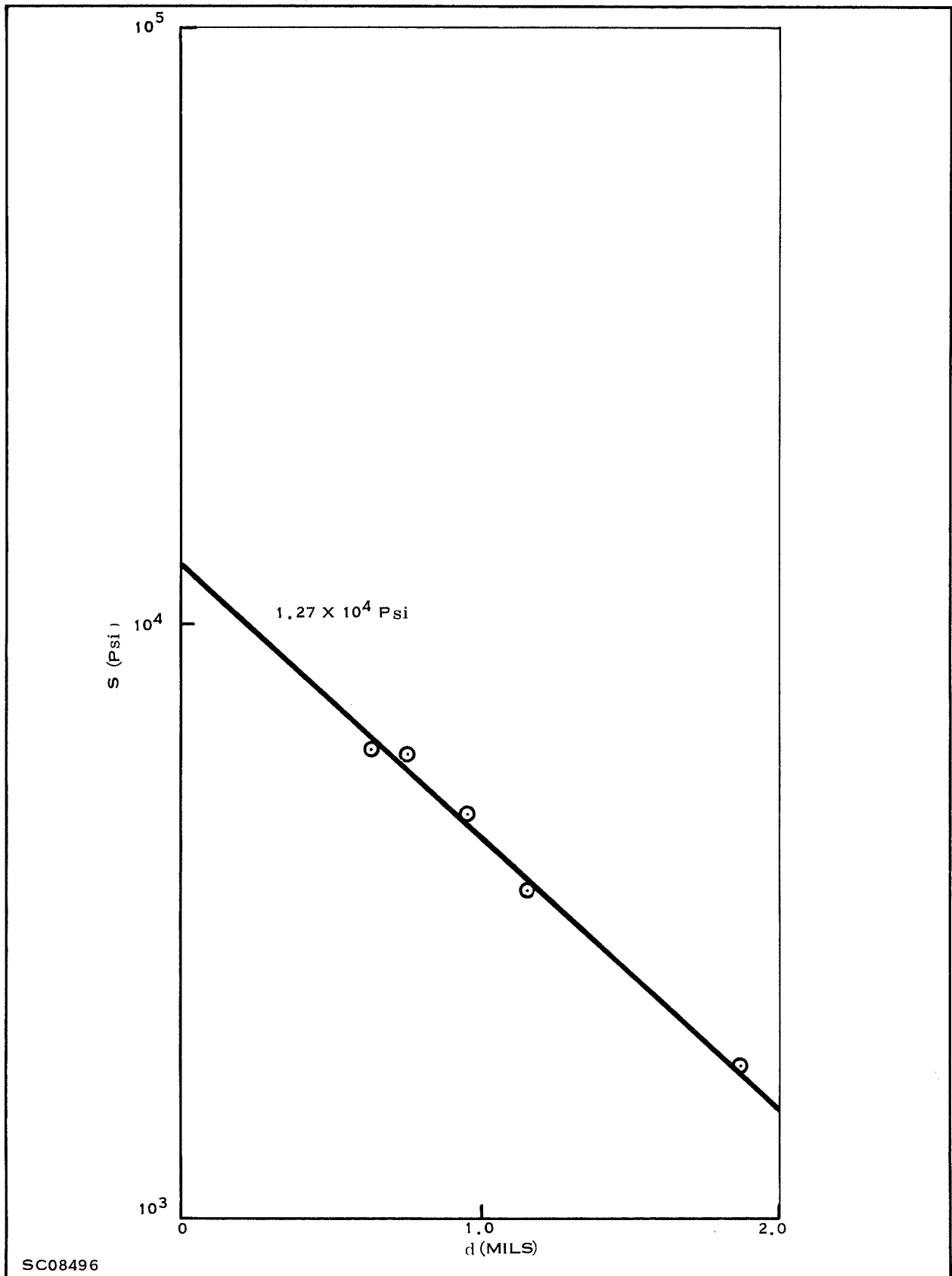


Figure 9. Stress versus Quartz-Film Thickness

decreases as deposit thickness increases. This suggests that some sort of stress-relief mechanism—possibly an annealing of oxide near the interface by continued sputtering—is in operation.

While further experiments would be required to detail the exact nature of the stresses in RF-sputtered films, these results clearly show that the maximum stresses involved ( $\cong 10^4$  psi) are much less than the compressive strength of  $\text{SiO}_2$  ( $> 1.6 \times 10^5$  psi), and the mechanical integrity of the films should be excellent.

### C. ANTI-REFLECTIVE COATINGS

In certain optical devices such as solar cells, anti-reflective coatings are utilized to minimize reflection, that is, losses at interfaces of different indices of refraction.

Although a thorough discussion on quarter-wavelength anti-reflection coatings will not be presented in this report, the basic requirements are provided for discussion. An anti-reflective coating for silicon solar cells should meet the following requirements:

- 1) High transmission in region of interest (0.4 to 1.2 micron).
- 2) Easily deposited at substrate temperatures less than  $350^\circ\text{C}$ .
- 3) Hard and adherent in deposited form.
- 4) Insoluble in normal solvents (water, acetone, etc.).
- 5) Proper index of refraction.

Silicon monoxide readily meets all the requirements outlined when it is used as the A-R coating between silicon and air (or conventional adhesives). The index of refraction of evaporated silicon monoxide coatings can be varied between 1.5 and 2.0 by controlling evaporation rate and oxygen pressure during deposition.<sup>13/</sup> Ideally, the silicon monoxide coating should have a refractive index of 1.87 for minimum reflectivity between silicon and air.

In general, for a quarter-wavelength coating to have minimum reflectivity at normal incidence it must meet the following requirement for refractive index:

$$N_2 = \sqrt{N_1 N_3}$$

where  $N_2$  is the refractive index of the coating of optical thickness  $N_2 t$ ,  $N_1$  and  $N_3$  are the refractive indices of the medium and the substrate, respectively. For example:

$$\begin{aligned} N_3 &= N_{\text{silicon}} \cong 3.5 \\ N_1 &= N_{\text{air}} = 1.0 \\ N_2 &= N_{\text{silicon monoxide}} = \sqrt{N_1 N_3} = 1.87 \end{aligned}$$

Now, if an anti-reflective coating is desired between silicon and fused silica ( $\text{SiO}_2$ ,  $N = 1.54$ ), it must meet all the outlined requirements and have a refractive index of 2.32, which is  $\sqrt{(1.54)(3.5)}$ . Silicon monoxide is, therefore, a poor anti-reflective coating between the integral cover glass and silicon solar cell.

A number of materials, which meet the outlined requirements and exhibit this desired refractive index, have been investigated and reported. Gadolinium titanate ( $\text{Gd}_2\text{Ti}_2\text{O}_7$ ) reportedly<sup>14/</sup> has a refractive index of 2.34 and is transparent from  $0.4 \mu\text{m}$  to  $6 \mu\text{m}$ . Cerium dioxide, extensively investigated as an anti-reflective coating, exhibits the desired characteristics<sup>15/</sup> when properly deposited. Lanthanum oxide<sup>16/</sup> ( $\text{La}_2\text{O}_3$ ) and silicon nitride ( $\text{Si}_3\text{N}_4$ ) are also potential candidates for the subject anti-reflective coatings. Although the reported refractive index for both  $\text{La}_2\text{O}_3$  and  $\text{Si}_3\text{N}_4$  is 2.0, it probably can be increased to approximately 2.3 by altering certain deposition parameters, such as substrate-temperature deposition rate, ambient pressure, etc.\*

Silicon nitride and cerium dioxide will be evaluated during the second quarter of the contract, since sources for both are currently available at Texas Instruments. Gadolinium titanate, lanthanum oxide, and possibly other materials will be evaluated during the contract, since this anti-reflective coating is very critical to the final performance of the integrally glassed cell.

Magnesium fluoride ( $\text{MgF}_2$ ) is commonly used as the anti-reflective coating between the  $\text{SiO}_2$  layer and air. Since this coating has been extensively developed in the industry for standard quartz cover slides, work on this contract will be directed primarily at developing and testing the integral coating and the anti-reflective coating between the Si and the  $\text{SiO}_2$ .

#### D. ENVIRONMENTAL TESTING

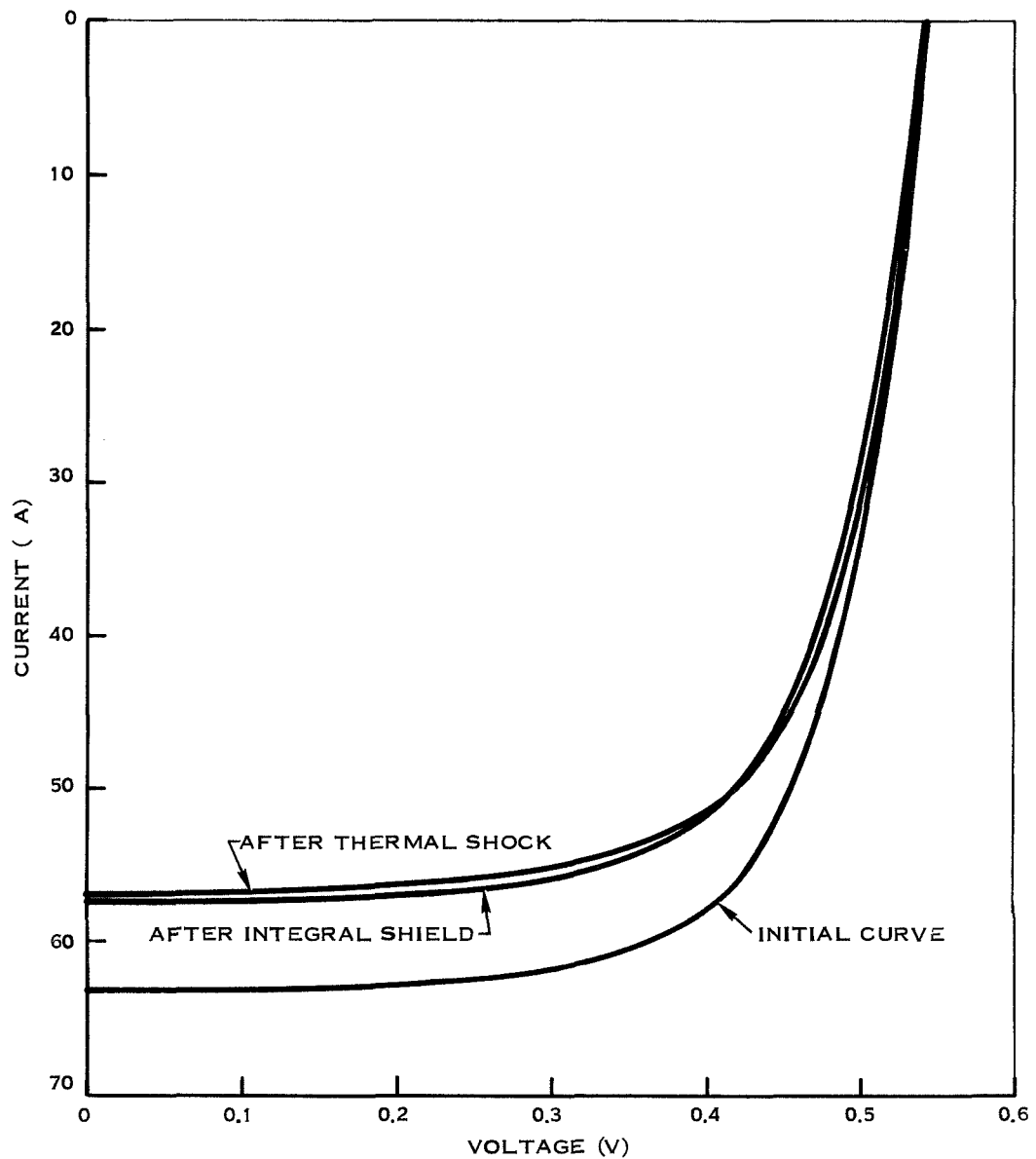
The contract requires that the environmental testing be performed on cells with 6-mil integral coatings; however, testing has been initiated on cells with 1-mil coatings. Additional testing will be performed as thicker coatings are developed. Since work during the first quarter of the contract was directed primarily at optimizing the deposition rate and uniformity of quartz, environmental testing on the program was scheduled to start the first month of the contract's second quarter. Temperature cycle and ultraviolet exposure tests are now in process on coatings deposited in May.

The temperature cycle consists of five cycles from  $+100$  to  $-100^\circ\text{C}$ . Integral cover glasses deposited by RF sputtering have survived thermal shock tests from boiling water to liquid nitrogen, as can be seen in Figure 10.

---

\* All the materials listed in this paragraph except silicon nitride can be evaporated from a tungsten boat. Silicon nitride can be reactively RF sputtered.





1 x 2 Cm, 3 GRID SOLDERLESS SOLAR CELL  
 100 mW/Cm<sup>2</sup> W  
 T<sub>C</sub> = 25°C  
 3 Cm H<sub>2</sub>O + 1/4" PLATE GLASS FILTER  
 SiO COATED PRIOR TO INTEGRAL SHIELD  
 BASE RESISTIVITY 7-14 Ω-Cm

THERMAL SHOCK: 5 CYCLES  
 LIQUID NITROGEN TO BOILING  
 WATER TO LIQUID NITROGEN  
 5 MINUTES AT EACH EXTREME.

THERMAL SHOCK AFTER INTEGRAL SHIELD APPLICATION

R-F SPUTTERED DEPOSIT OF  
 COMMERCIAL GRADE QUARTZ  
 THICKNESS 0.8 MILS

SC05239

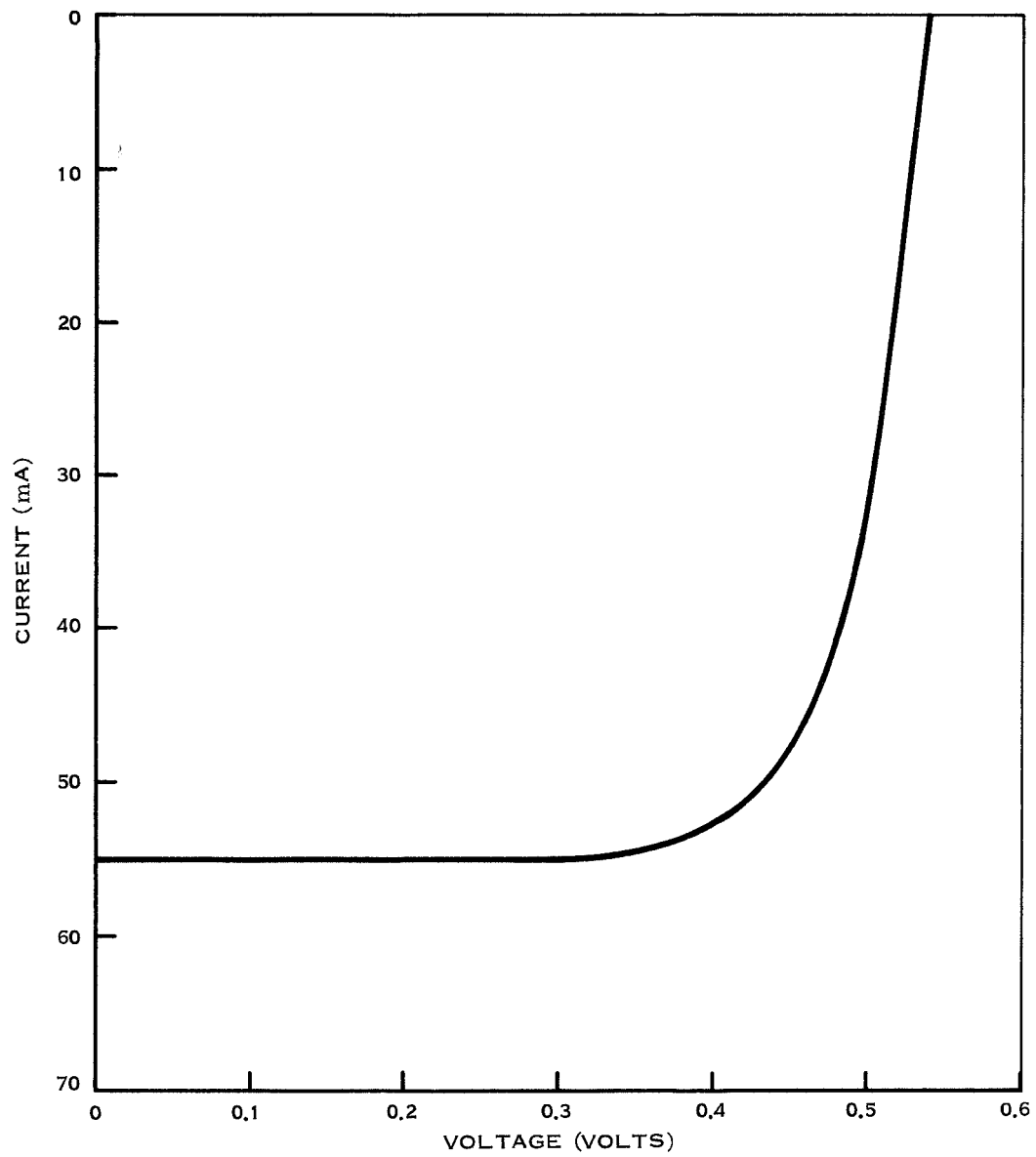
Figure 10. I-V Curve before and after Quartz Coating and after Thermal Shock

## E. SAMPLE FABRICATION

The five samples supplied for the first quarter of the contract consisted of the following:

- 1) Substrate: N/P silicon solar cell, 1 x 2 cm, three-grid, 7 to 14  $\Omega$  cm base resistivity, solderless contacts.
- 2) Anti-reflective coating (Si-SiO<sub>2</sub>): silicon monoxide.
- 3) Integral cover glass: Corning 7940 fused silica, 1 mil thickness.
- 4) Anti-reflective coating (SiO<sub>2</sub>-air): none.

Figure 11 is the I-E characteristic of sample cell No. 1. The light source was calibrated with a Table Mountain standard solar cell.



SC08941

Figure 11. Solar Cell I-E Characteristic After Integral Quartz Coating

### SECTION III

#### PROGRAM FOR NEXT THREE MONTHS

Work will continue on maximizing the deposition rate of quartz with the 6-inch-diameter cathode. Thicker coatings in the 1.5-to-3-mil range will be deposited and evaluated. Work will be initiated to develop a satisfactory anti-reflective coating between the solar cell and the integral quartz layer. Environmental testing will be initiated to evaluate coatings of from 1 to 3 mils thickness on temperature cycle and ultraviolet exposure. No problems are anticipated with the vacuum storage test, since the quartz is deposited in vacuum and is a chemically stable material.

## SECTION IV

### CONCLUSIONS

Integral quartz layers up to 3.5 mils thick have been successfully deposited on solar cells by radio-frequency sputtering. Radio-frequency sputtering promises to be an excellent technique for depositing integral cover-glass layers directly on silicon solar cells for the following reasons: (1) low-stress, high-adherent films can be deposited at high deposition rates ( $> 2000 \text{ \AA}/\text{min}$  for  $\text{SiO}_2$ ); (2) substrate temperature is less than  $200^\circ\text{C}$  during deposition. One-mil-thick coatings have successfully passed thermal shock from liquid nitrogen to boiling water for five cycles with no delamination or degradation. The stress of RF-sputtered quartz films deposited on silicon solar cells has been measured and reported.

Quartz coatings deposited directly on silicon monoxide coated cells yielded approximately 10 percent decrease in output current of the cell under tungsten light. This loss can be attributed to reflection losses at the quartz-air interfaces and at the Si-SiO-SiO<sub>2</sub> interfaces. However, even with these unoptimized conditions, integrally coated,  $10 \text{ } \Omega \text{ cm}$  base resistivity N/P solar cells have been fabricated with final conversion efficiency of approximately 10 percent AMO.

## SECTION V

### REFERENCES

1. Fang, P. F., Proceedings of the Fifth Photovoltaic Specialists Conference (October, 1965).
2. Smith, K. D.; Gummel, J. D.; Bode, J. D.; Cuttriss, D. B.; Nielson, R. J., and Rosenweig, "The Solar Cells and Their Mountings," Bell System Technical Journal, Vol. XLII, No. 4 (July, 1963).
3. Marks, B. S., "Solar Cell Coatings," Proceedings of the Fifth Photovoltaic Specialists Conference, Vol. I, B-5 (October, 1965).
4. Second Quarterly Report, Solar Cell Cover Glass Development, Contract No. NAS 5-10236, 13 (1966).
5. Anderson, G. S.; Mayer, Wm. N.; and Wehner, G. K.; "Sputtering of Dielectrics by High-Frequency Fields," Journal of Applied Physics, 33, 10, 2991-2992 (October, 1962).
6. Butler, H. S., and Kino, G. S., "Plasma Sheath Formation by Radio-Frequency Fields," Physics of Fluids, 6, 9, 1346-1355 (September, 1963).
7. "R-F Sputtered Insulators Protect Integrated Circuits," Electronic News, 4 (July 5, 1965).
8. Davidse, P. D., and Maissel, L. I., "R-F Sputtering of Insulators," IBM Systems Development Division, Poughkeepsie, N. Y.
9. Stuart, R. V., and Wehner, G. K., "Sputtering Yields for Low Energy  $\text{Ar}^+$ - and  $\text{Ne}^+$ -Ion Bombardment," Journal of Applied Physics, 33, 2345 (1962).
10. Rosenbery, D., and Wehner, G. K., "Sputtering Yields for Low Energy  $\text{He}^+$ - $\text{Kr}^+$ -, and  $\text{Xe}^+$ -Ion Bombardment," Journal of Applied Physics, 33, 1842 (1962).
11. Brenner, A., and Senderoff, V. Res., NBS, 42, 105 (1949).
12. Stoney, G. G., Proc. Roy. Soc. (London) (A), 82, 172 (1909).
13. Drumkeller, C. E., "Properties and Application of Silicon Monoxide," Kemet Co., Cleveland, Ohio (1960).
14. Merker, L., and Herrington, K. D., Appl. Opt. 3, 1311 (1964).
15. Hass, G.; Ramsey, J. B., and Thun, R., Jour., Optical Society of Amer., 48, 324 (1958).
16. Laikin, M., Appl. Opt., 4, 1032 (1965).